Journal of Advanced Research 51 (2023) 135–147

Contents lists available at ScienceDirect

Journal of Advanced Research

journal homepage: www.elsevier.com/locate/jare

Original Article

Targeting ARF1-IQGAP1 interaction to suppress colorectal cancer metastasis and vemurafenib resistance

Hui-Fang Hu [a,b], Gui-Bin Gao [b], Xuan He [b], Yu-Ying Li [b], Yang-Jia Li [b], Bin Li [b], YunLong Pan [a,*], Yang Wang [b,*], Qing-Yu He [a,b,*]

[a] The First Affiliated Hospital of Jinan University, Jinan University, Guangzhou 510632, China
[b] MOE Key Laboratory of Tumor Molecular Biology and Key Laboratory of Functional Protein Research of Guangdong Higher Education Institutes, Institute of Life and Health Engineering, College of Life Science and Technology, Jinan University, Guangzhou 510632, China

HIGHLIGHTS

- ARF1 is upregulated in both metastatic CRC and vemurafenib-resistant CRC cells.
- ARF1 promotes CRC metastasis and vemurafenib resistance by interacting with IQGAP1.
- ARF1-IQGAP1 interaction induces ERK pathway reactivation in vemurafenib resistance.
- LY2839219 suppresses CRC metastasis by disturbing ARF1-IQGAP1 interaction.
- Combination of LY2835219 and vemurafenib is a promising strategy for CRC treatment.

GRAPHICAL ABSTRACT

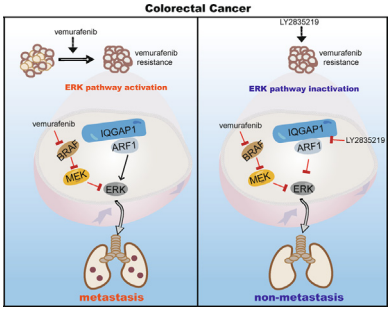

ARTICLE INFO

Article history:
Received 12 July 2022
Revised 11 October 2022
Accepted 10 November 2022
Available online 14 November 2022

Keywords:
Colorectal cancer
Vemurafenib resistance
Metastasis
LY2835219
ARF1-IQGAP1 interaction

ABSTRACT

Introduction: Acquired resistance to BRAF inhibitor vemurafenib is frequently observed in metastatic colorectal cancer (CRC), and it is a thorny issue that results in treatment failure. As adaptive responses for vemurafenib treatment, a series of cellular bypasses are response for the adaptive feedback reactivation of ERK signaling, which warrant further investigation.
Objectives: We identified ARF1 (ADP-ribosylation factor 1) as a novel regulator of both vemurafenib resistance and cancer metastasis, its molecular mechanism and potential inhibitor were investigated in this study.
Methods: DIA-based quantitative proteomics and RNA-seq were performed to systematic analyze the profiling of vemurafenib-resistant RKO cells (RKO-VR) and highly invasive RKO cells (RKO-I8), respectively. Co immunoprecipitation assay was performed to detect the interaction of ARF1 and IQGAP1 (IQ-domain GTPase activating protein 1). An ELISA-based drug screen system on FDA-approved drug library was established to screen the compounds against the interaction of ARF1-IQGAP1.The biological functions of ARF1 and LY2835219 were determined by transwell, western blotting, Annexin V-FITC/PI staining and *in vivo* experimental metastasis assays.
Results: We found that ARF1 strongly interacted with IQGAP1 to activate ERK signaling in VR and I8 CRC cells. Deletion of IQGAP1 or inactivation of ARF1 (ARF-T48S) restored the invasive ability induced by ARF1. As ARF1-IQGAP1 interaction is essential for ERK activation, we screened LY2835219 as novel inhibitor of ARF1-IQGAP1 interaction, which inactivated ERK signaling and suppressed CRC metastasis and

Peer review under responsibility of Cairo University.
* Corresponding authors at: Institute of Life and Health Engineering, College of Life Science and Technology, Jinan University, Guangzhou 510632, China.
E-mail addresses: tpanyl@jnu.edu.cn (Y. Pan), wangyang0507@jnu.edu.cn (Y. Wang), tqyhe@jnu.edu.cn (Q.-Y. He).

https://doi.org/10.1016/j.jare.2022.11.006

vemurafenib-resistance *in vitro* and *in vivo* with no observed side effect. Furthermore, LY2835219 in combined treatment with vemurafenib exerted significantly inhibitory effect on ARF1-mediated cancer metastasis than used independently.

Conclusion: This study uncovers that ARF1-IQGAP1 interaction-mediated ERK signaling reactivation is critical for vemurafenib resistance and cancer metastasis, and that LY2835219 is a promising therapeutic agent for CRC both as a single agent and in combination with vemurafenib.

Introduction

Colorectal cancer (CRC) is the third most common cancer worldwide, accounting for the second highest cancer-related mortality [1–3]. More than 45 % of CRC patients are first diagnosed with metastasis due to the concealed symptoms and the tumor aggressiveness [4]. Currently, the existing chemotherapies for CRC are bottlenecked by their toxic effects or low efficiency against distant metastatic cancer cells, which are the key reasons for treatment failure and cancer-related death. Drug-resistance and metastasis are linked phenomena during the progression of cancer evolution [5], there is an urgent need to develop more effective and low toxicity drugs for CRC therapy against drug-resistance and cancer metastasis.

BRAF is a crucial player in MAPK/ERK signaling. BRAF mutation (V600E)-induced continuous activation of MAPK/ERK signaling is frequently observed in CRC patients with poor prognosis [6]. Vemurafenib is an FDA-approved BRAF inhibitor that exerts a favorable therapeutic efficacy on unrespectable melanoma with BRAF-V600 mutation [7,8]. However, vemurafenib shows a limited effect on CRC [9] because of the existence of receptor tyrosine kinases (RTKs), such as EGFR. Long-term treatment of vemurafenib in CRC cells with BRAF-V600E induces the reactivation of MEK/ERK signaling [10], suggesting that a series of potential bypasses are activated for adaption to vemurafenib. In our established vemurafenib-resistant (VR) CRC cell line (RKO-VR), high invasive capacity was found as compared to its parental cells. To explore the mechanism of vemurafenib-mediated resistance and cancer metastasis in CRC, we analyzed differentially expressed proteins/genes (DEPs/DEGs) in RKO-VR and high-invasive CRC cell line (RKO-I8) *versus* controls by DIA-based quantitative proteomics and RNA sequencing. ADP-ribosylation factor 1 (ARF1)-mediated ERK signaling network was highly activated in both the RKO-VR and RKO-I8 CRC cells, which led us to hypothesize that targeting ARF1-mediated ERK signaling may be able to overcome vemurafenib resistance and metastasis.

ARF1 is a member of highly conserved Ras family, and its GTPase activity is closely related to cancer metastasis, in which it exchanges from inactive (GDP bound) to active (GTP bound) conformation [11–13]. ARF1 was reported to induce drug resistance *via* activating ERK and AKT signaling pathway in myeloma [14]. As a GTPase activator, IQ motif containing GTPase activating protein 1 (IQGAP1) was previously demonstrated to bind with ARF1 to promote ERK signaling activation and CRC growth [15]. In this study, we revealed the critical role of ARF1-IQGAP1 interaction in vemurafenib resistance and cancer metastasis.

In addition, we previously developed an enzyme-linked immunosorbent assay (ELISA)-based screening system for seeking molecular compounds that interrupt protein–protein interactions [16]. Based on this strategy, we here identified LY2835219 from an FDA-approved drug library containing 88 molecules as a novel inhibitor targeting ARF1-IQGAP1 interaction. LY2835219, a cyclin-dependent kinase (CDK) 4/6 inhibitor, inhibits retinoblastoma (Rb) protein signaling to prevent cell cycle progression from G1 to S phase [17]. Though LY2835219 was reported to exhibit anticancer effect on breast cancer [18], its effect on CRC remains unclear. In our study, *in vitro* and *in vivo* experiments were performed to investigate the effects of LY2835219 on CRC related to vemurafenib resistance and cancer metastasis. We also assessed whether targeting ARF1-IQGAP1 interaction with LY2835219 enhances the anti-metastasis efficacy of vemurafenib on CRC.

Materials and Methods

Ethics statement

All experiments involving animals were conducted according to the ethical policies and procedures approved by the Ethics Committee for Animal Experiments of Jinan University (Approval no. 20201020–05).

Cell lines and drugs

The human colorectal cancer cell lines HCT116, RKO, DLD1 and HT29 (ATCC, Rockville, MD, USA) were cultured in RPMI 1640 medium (Life Technologies, Gaithersburg, MD, USA) containing 10 % fetal bovine serum (Life Technologies). The stable cells with ARF1-overexpression, ARF1-knockdown and IQGAP1-knockout were constructed in our previous study [15]. RKO-VR cells were screened using high-concentration (100 μM) vemurafenib. The high-invasive cell lines (I8 cells) were established in our previous study [19]. Vemurafenib, LY2835219 and U0126 were purchased from Selleck (Huston, TX, USA).

Transwell assay

The method of transwell assay was described previously [19,20]. Briefly, the matrigel (BD Bioscience, Bedford, MA, USA) was diluted with medium (1:20), and spread evenly on the chamber for 1 h at 37 °C. Then the cells suspended in serum-free medium were added to the upper chamber, and medium containing 10 % FBS was filled in the lower chamber. After 24 h, the chamber was collected and fixed with methanol for 15 min. The images of chamber were captured and quantified after staining with 2 % crystal violet.

Quantitative real-time PCR (qRT-PCR)

HiPure Total RNA Kits (Magen, Guangzhou, China) was used to extract the total RNA of cells, and PrimeScript II first Strand cDNA Synthesis Kit (Takara, Dalian, China) was used to perform reverse transcription. SYBR Premix Ex *Taq*II (Takara) was used to analyze the mRNA expression of ARF1 and internal control GAPDH on a Mini Option real-time PCR system (Bio-Rad). The primers sets: forward, 5′-GAAGGTGAAGGTCGGAGTC-3′, reverse, 5′-AAGATGGT GATGGGATTTC-3′ for GAPDH. forward, 5′-GACCACCATTCCCACCA TAG-3′, reverse, 5′-GAACACCAGGAGGACAGCAT-3′ for ARF1.

Western blotting

The lysates of cells with indicated treatment were extracted by cell lysis (Cell Signaling Technology, Beverly, MA, USA) and the

protein concentrations were quantified by using a BCA kit (Thermo Fisher Scientific, San Jose, CA, USA). The equal amount of protein was mixed with loading buffer and boiled at 95 °C for 5 min. After separating by SDS-PAGE, the protein was transferred to a PVDF membrane and blocked with 5 % milk for 2 h. The membrane was then incubated with primary antibody overnight at 4 °C, and followed with incubation of corresponding secondary antibody at room temperature for 1 h. The protein signal on membrane was visualized by autoradiographic film (Tanon-5200Multi, Bio-Technologyco.ltd, Guangzhou, China). Primary antibodies included actin, ERK, p-ERK, ARF1 were obtained from Proteintech (Wuhan, China).

Purification of ARF1-His and IQGAP1-GST proteins

As previously described [15], the expression plasmids of pET28b-ARF1 and pGEX-4 T-1-IQGAP1 were constructed and transformed into E. coli BL21 star cells for expression, respectively. The bacteria were cultured in LB medium at 37 °C until the optical density at 600 nm reached 0.6, 0.5 mM isopropyl β-D-thiogalactopyranoside (IPTG) was added for 12 h to induce protein expression. Finally, the bacteria were collected and lysed by sonication, and the fusion ARF1-His and IQGAP1-GST proteins were isolated using His/GST-binding column (Beyotime Biotechnology, Shanghai, China).

ARF1 activity assay

ARF1 Activation Assay Kit (Abcam, ab211170) was used to determine the ARF1 activity according to the manufacturer's instruction. GGA3 PBD Agarose beads was used to selectively isolate and pull-down the active form of ARF1 from cell lysates. Subsequently, Western blotting assay was used to detect the GTP-ARF1 using an anti-ARF1 antibody.

ELISA-based drug screen system

The first layer GST-tag antibody was diluted to 1 ng/μL with coating buffer, and added into the ELISA 96-well plate for incubation overnight at 4 °C. After washing with PBS for three times, the 5 % bovine serum albumin (BSA) was added into the 96-well plate for 2 h at 37 °C. For the second layer, fusion protein IQGAP1-GST (2 μg) was added into the plate and incubated for 4 h at room temperature. The plate washed with PBS was added with the third layer fusion protein ARF1-His (2 μg) and the individual small molecular drugs, followed by incubation at 37 °C for 3 h. After washing with PBS, the diluted his-tag antibody (1:1000) was added into the well and incubated 2 h at room temperature. The plate was then washed and incubated with horseradish peroxidase (HRP) labeled goat-anti-rabbit antibody (1:2000 in 5 % BSA; Abcam, Cambridge, MA, UK) for 1.5 h at room temperature. The 96-well plate was added with 100 μL tetramethylbenzidine (TMB) and cultured for 1 min at 37 °C, followed by adding termination buffer 50 μL into the well quickly. At the end of experiment, the absorbance at 450 nm and 630 nm was measured, and OD450-OD630 was used to analyze the level of IQGAP1-ARF1 interaction.

Co-immunoprecipitation (Co-IP)

The cells or CRC tissues were collected in the IP lysis buffer (Cell Signaling Technology), then the lysates were incubated with IgG (Santa Cruz Biotechnology, Santa Cruz, CA, USA) and protein A/G Sepharose beads (Invitrogen, Gaithersburg, MD, USA) at 4 °C for 1 h. The supernatant was collected and incubated with primary antibodies at 4 °C overnight, protein A/G Sepharose beads were added into cell lysates for 4 h of incubation. After washing with IP lysis buffer and PBS for three times, the beads were mixed with loading buffer for western blotting analysis.

Cell viability assay

The WST-1 cell proliferation and cytotoxicity assay kit (Beyotime Biotechnology) was used to measure the cell viability according to the manufacturer's instruction. In brief, the cells were seeded into the 96-well plate for indicated treatment, and then added with WST-1 for incubation 3 h at 37 °C. An automated microplate spectrophotometer (BioTek Instruments, Winooski, VT, USA) was used to measure the absorbance at 450 nm.

Annexin V-FITC/PI staining assay

The Annexin V-FITC/PI Apoptosis Detection kit (KeyGen, Jiangsu, China) was used to analyze cell apoptosis. In brief, cells were stained with annexin V-FITC and propidium iodide (PI) for 20 min, then BD FACSCelesta™ Flow Cytometer (BD Biosciences, San Diego, CA) was used to analyze the apoptotic cells.

Transfection

The siRNA against CDK4 (CTGACTTTTAACCCACACA) and CDK6 (TACTTCTGAAGTGTTTGACATTT) was obtained from TransheepBio (Shanghai, China). The siRNA against ARF1 and pcDNA3.1-ARF1 plasmid were constructed as previously described [15]. For transfection, Lipofectamine 3000 reagent (Thermo Fisher Scientific) was used according to the manufacturer's instruction.

RNA-sequence

HiPure Unviersal RNA Mini Kit (Magen Biotechnology Co., ltd, Guangzhou, China) was used to extract RNA, and sequenced by Illumina Hiseq X Ten sequencer. The result was analyzed by using FANSe3 algorithm, in detail, passed the Illumina quality filters were matched to the human mRNA reference database on Chi-Cloud NGS Analysis Platform (Chi-Biotech Co. ltd., Shenzhen, China).

Mass spectrometry (DIA) and bioinformatics analyses

Protein digestion and mass spectrometric analysis were executed as previously described [21]. In brief, RKO-VR and parental cells were lysed with SDS lysis buffer (Beyotime Biotechnology). Protein was digested with trypsin (Promega, Fitchburg, WI, USA), vacuum-freeze-dried and resuspended in anhydrous acetonitrile solution, then desalted with MonoTIPTM C18 Pipette Tip (GL Sciences, Tokyo, Japan). Peptide samples were analyzed with an Orbitrap Fusion Lumos mass spectrometer (Thermo Fisher Scientific). Proteome Discoverer (Thermo Fisher Scientific) was used to analyze the raw data. Protein and peptide FDRs were set to 1 %. Kyoto Encyclopedia of Genes and Genomes (KEGG, https://www.kegg.jp) was used to analyze the differentially expressed proteins (DEPs).

In vivo experimental metastasis model and drug treatment

Female NOD-Prkdc^{em26Cd52}Il2rg^{em26Cd22} (NCG) mice (GemPharmatech Co., ltd Jiangsu, China) aged 6–8 weeks were cared according to the guidelines for the care and use of animal experiments, and were approved by the Ethics Committee for Animal Experiments of Jinan University. The method for experimental metastasis model was described previously [22,23]. In brief, the cells suspended in PBS were injected intravenously into NCG mice (100 μL/mice). After two weeks of observation, the metastasis of

cancer cells was visualized by bioluminescent imaging (Xenogen IVIS lumima II, PerkinElmer, MA, USA), and analyzed by the Living Image R Software Version3.1. For the drug treatment experiments, the NCG mice injected with cancer cells were divided into treatment group and control group, the treatment groups received oral gavage of drugs, whereas the control group received vehicle, and the signal of metastasis of cancer cells was observed by bioluminescent imaging. At the end of the experiment, the lungs were harvested for H&E staining, and the serum alanine aminotransferase (ALT) and aspartate aminotransferase (AST) were analyzed.

Statistical analysis

All *in vitro* assays were performed three times, and all data were expressed as the mean ± SD and statistically significant differences were calculated with *t*-test. $P < 0.05$ was considered statistically significant. The datasets with survival data from patients with colorectal cancer were downloaded from the GEO database (GSE17536) and Clinical Proteomic Tumor Analysis Consortium (CPTAC, PDC000116). The association between ARF1 expression and survival of patients was analyzed by Kaplan-Meier method, and the log-rank test was used to compare the statistical difference. Bars, SD; $^{*}P < 0.05$; $^{**}P < 0.01$; $^{***}P < 0.001$; ns, no significant difference.

Results

Identification of ERK signaling and ARF1 as key drivers of vemurafenib resistance and CRC invasion

Persistent treatment with BRAF inhibitor vemurafenib on CRC rapidly induces ERK reactivation through epidermal growth factor receptor (EGFR) [10], we thus speculated that a series of cellular bypasses are activated for the adaptive resistance. Herein, we generated vemurafenib-resistant RKO cell line (RKO-VR) by continuous treatment with vemurafenib (100 μM; Fig. 1A) for weeks. The established RKO-VR cell line was confirmed by the WST-1 and the annexin V-FITC/PI double-staining assay (Fig. S1A, B). Interestingly, we found that RKO-VR cells exhibited higher invasive capacity than parental RKO cells (Fig. 1B). In addition, RKO-VR cells showed refractory to vemurafenib-mediated inhibitory effects on cell invasion (Fig. 1C). In order to screen for novel regulators involved in VR-associated metastasis, we employed previously established highly invasive CRC sublines (RKO-I8 and HCT116-I8) [24], showing significantly higher invasion ability than their parental cell lines (Fig. 1D, E). We then performed DIA-based proteomics (Table S1) and global RNA sequencing (Table S2) to determine DEPs/DEGs in vemurafenib-resistant cells (RKO-VR *vs* RKO) and high invasion cells (RKO-I8 *vs* RKO), respectively. A total of 1356 proteins were differentially expressed in RKO-VR and 2079 DEGs were identified in RKO-I8 (Fig. S1C). KEGG pathway analysis of these DEPs/DEGs revealed that MAPK signaling pathway was significantly enriched in RKO-VR and RKO-I8 (Fig. 1F, G), suggesting that MAPK signaling is involved in the VR-associated cancer metastasis. To identify the co-regulators of VR-associated metastasis that are functionally relevant to MAPK signaling, the upregulated proteins/genes in RKO-VR and RKO-I8 were overlapped (Table S3). A total of 73 candidates were identified and subjected to literature mining for their function on MAPK signaling. ADP ribosylation factor 1 (ARF1), a small guanine nucleotide-binding protein that was reported to activate ERK by binding with IQGAP1 [15], was significantly upregulated in both RKO-VR and RKO-I8 (Fig. 1H). Our following qRT-PCR and Western blotting confirmed that the expression of ARF1, as well as p-ERK, was increased in HCT116-I8, RKO-VR and RKO-I8 cells (Fig. 1I-K), as compared to corresponding parental cell lines.

To assess the clinical significance of ARF1 in CRC, we analyzed the data from the Clinical Proteomic Tumor Analysis Consortium (CPTAC) and found that ARF1 expression was significantly higher in CRC tissues compared to corresponding normal tissues (Figure S2A), and was positively correlated with advanced clinical stages (III-IV) ($P = 0.031$; Fig. S2B). The Receiver operating characteristic (ROC) curve illustrated that ARF1 could be used as a diagnostic marker for CRC with AUC value of 0.743 (Fig. S2C). We divided CRC patients (CPTAC, ID: PDC000116) into two groups according to ARF1 expression, and found that patients with ARF1-high had higher risk to be poor prognosis (Fig. S2D, E). The result was further confirmed by Kaplan-Meier analysis of another cohort (GSE17536), showing that patients with high ARF1 expression had markedly shorter survival (Fig. S2F, G). By detecting ARF1 level in clinical CRC tissues, we found that ARF1 was highly expressed in primary tumors (T3/4 stage) and metastatic tumors (N and M stage) of CRC, as compared to primary tumors with T1/2 stage (Fig. S2H). These results suggested that ARF1 is associated with the advanced tumor stages and metastasis, serving as a potential biomarker for the prognosis of CRC.

ARF1 promotes CRC metastasis and vemurafenib resistance

To explore the molecular function of ARF1 in CRC metastasis and vemurafenib resistance, we established ARF1-overexpression and ARF1-knocdown stable cell lines (Figure S3A) in various CRC cell lines. We then found that HCT116 and RKO cells with ARF1 overexpression had higher invasive ability than control cells (Fig. 2A), while knockdown of ARF1 in DLD1, HT29, HCT116-I8 and RKO-I8 remarkably decreased invasion ability of CRC cells (Fig. 2B and Figure S3B). In addition, we established an *in vivo* CRC metastasis model by intravenous injection of HCT116-Luc or HCT116-Luc-ARF1 cells into the tail vein of NCG mice, and validated the effect of cell metastasis by bioluminescence imaging (Fig. 2C). We observed that ARF1 significantly promoted lung metastasis (Fig. 2C), as evidenced by H&E staining of metastatic nodes in collected lung (Fig. 2D). Furthermore, we found that ARF1 overexpression in HCT116 and RKO significantly reversed the anticancer effects of vemurafenib (48–72 h, 10 μM), as evidenced by CCK-8 and Annexin V/PI assays (Fig. S3C, D). On the contrary, knockdown of ARF1 with siRNA in RKO-VR cells (Fig. 2G) improved the anticancer effect of vemurafenib (Figure S3E, F). In addition, we found that overexpression ARF1 conferred CRC cell resistance to vemurafenib mediated anti-metastasis effect and p-ERK inactivation (Fig. 2E, F, I), while knockdown of ARF1 expression remarkably enhanced the anti-metastasis effect of vemurafenib and p-ERK inactivation (Fig. 2H, J) within short time treatment (24 h). Taken together, ARF1 is an important mediator in vemurafenib resistance and metastasis of CRC.

ARF1 promotes metastasis and vemurafenib resistance by activating MAPK/ERK signaling

Our above experiments revealed that MAPK signaling plays a chief role in ARF1-involved CRC metastasis and vemurafenib resistance. To confirm this result, we introduced U0126 (a specific MEK/ERK inhibitor) and found that the invasive ability of HCT116 and RKO promoted by ARF1, even in the condition of vemurafenib treatment, could be abolished by U0126 (Fig. 3A, B). We previously reported that ARF1 promoted ERK signaling mediated tumorigenesis *via* binding with IQGAP1 [15]. Here, our Co-IP assay revealed that the interaction of ARF1-IQGAP1 was markedly increased in I8 and VR cells, as compared to their corresponding parental cells (Fig. 3C). Among these cells, no obvious difference was found in

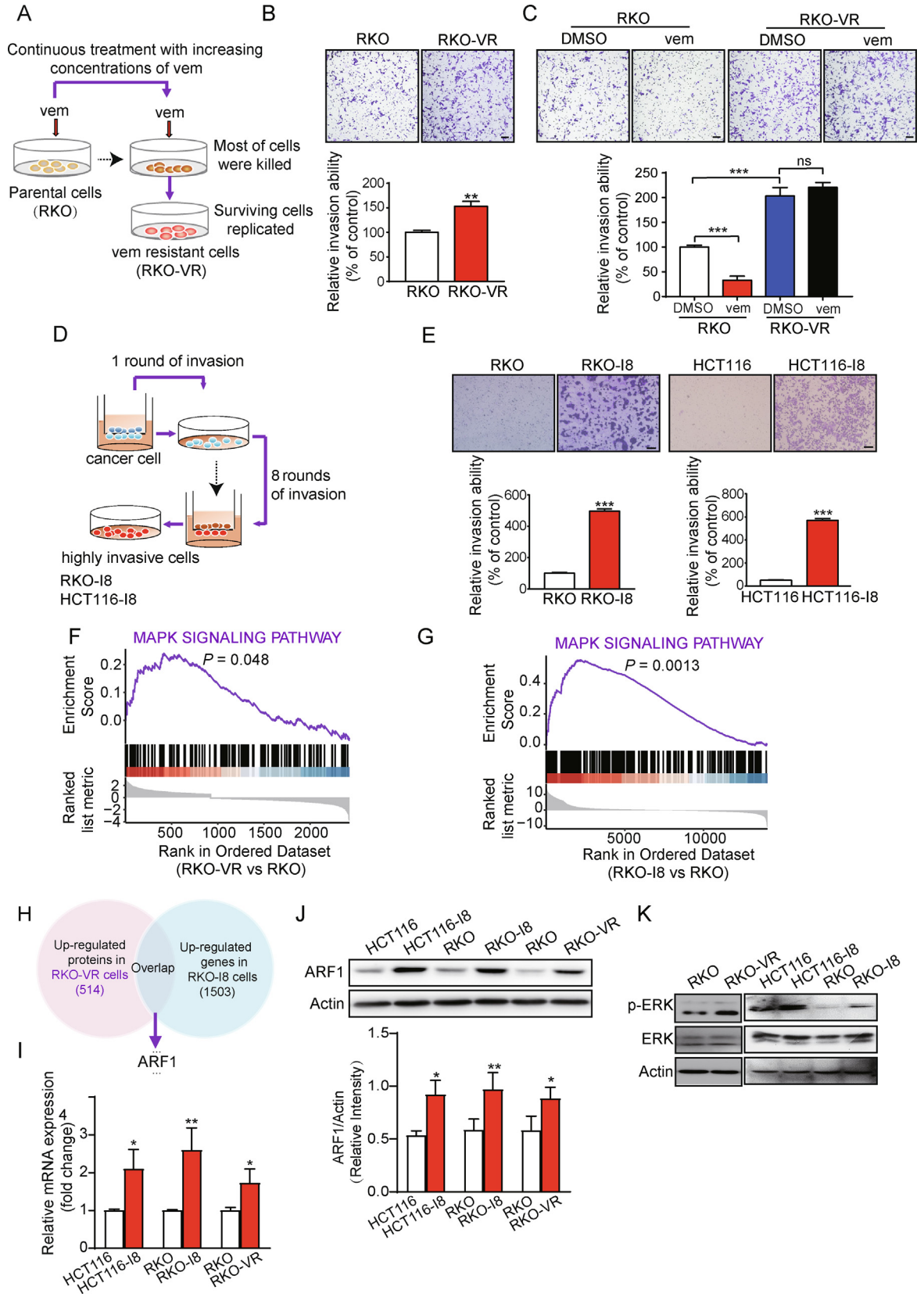
A
Continuous treatment with increasing concentrations of vem
vem
vem
Most of cells were killed
Parental cells (RKO)
Surviving cells replicated
vem resistant cells (RKO-VR)
B
RKO
RKO-VR
Relative invasion ability (% of control)
RKO RKO-VR
C
RKO
RKO-VR
DMSO
vem
DMSO
vem
Relative invasion ability (% of control)
ns
DMSO vem DMSO vem
RKO
RKO-VR
D
1 round of invasion
cancer cell
8 rounds of invasion
highly invasive cells
RKO-I8
HCT116-I8
E
RKO
RKO-I8
HCT116
HCT116-I8
Relative invasion ability (% of control)
RKO RKO-I8
HCT116 HCT116-I8
F
MAPK SIGNALING PATHWAY
P = 0.048
Enrichment Score
Ranked list metric
Rank in Ordered Dataset (RKO-VR vs RKO)
G
MAPK SIGNALING PATHWAY
P = 0.0013
Enrichment Score
Ranked list metric
Rank in Ordered Dataset (RKO-I8 vs RKO)
H
Up-regulated proteins in RKO-VR cells (514)
Overlap
Up-regulated genes in RKO-I8 cells (1503)
ARF1
I
Relative mRNA expression (fold change)
HCT116 HCT116-I8 RKO RKO-I8 RKO RKO-VR
J
HCT116 HCT116-I8 RKO RKO-I8 RKO RKO-VR
ARF1
Actin
ARF1/Actin (Relative Intensity)
HCT116 HCT116-I8 RKO RKO-I8 RKO RKO-VR
K
RKO RKO-VR HCT116 HCT116-I8 RKO RKO-I8
p-ERK
ERK
Actin

the IQGAP1 expression (Figure S4A). Moreover, the interaction of ARF1 and IQGAP1 was detected in clinical CRC tissues with BRAF V600E mutation (case#1, case#2, case#3) and BRAF wild type (case#4, case#5, case#6) (Fig. S4B), suggesting that highly activated ARF1-IQGAP1 interaction is important for MAPK/ERK signaling activation and vemurafenib resistance. In addition, we overexpressed ARF1 in IQGAP1-kncokout cells, and found that ectopic ARF1 expression could not promote the invasive ability of CRC in IQGAP1-knockout cells (Fig. 3D). Since Thr-48 of ARF1 plays an important role in its activation and interaction with IQGAP1 [25,26], we confirmed that ARF1 with the mutation of Thr-48 to Ser impaired its activation (Figure S5A), showing no effect on cell invasion and ERK activation and loss of the affinity with IQGAP1 in CRC cells (Fig. 3E, S5B-C). Collectively, these results demonstrated that ARF1-IQGAP1 interaction mediated ERK signaling is critical for CRC metastasis and vemurafenib resistance.

LY2839219 blocks ARF1-IQGAP1 interaction

Regarding the crucial role of ARF1-IQGAP1 interaction in MAPK/ERK signaling pathway, we developed an ELISA-based drugs screen system (Fig. 4A) to screen for small molecule inhibitors that potently suppress ERK signaling activation through disrupting ARF1-IQGAP1 interaction. By using an FDA-approved library consisting of 88 compounds, we identified LY2839219 that exhibited suppressive effect on ARF1-IQGAP1 interaction (Fig. 4B, C). To confirm this result, HCT116 and RKO cells were treated with LY2839219, and Co-IP assays were carried out to verify the effect on ARF1-IQGAP1 interaction. As shown in Fig. 4D-E, LY2839219 significantly disrupted the ARF1-IQGAP1 interaction in both HCT116, RKO and RKO-VR cells in a dose-dependent manner. Furthermore, our results demonstrated that LY2839219 suppressed p-ERK activation in a dose-dependent manner, but not influence the protein levels of IQGAP1 and ARF1 (Fig. 4F). These results prove that LY2839219 targets the ARF1-IQGAP1 interaction to inactivate ERK in CRC cells.

LY2839219 suppresses cancer metastasis by disrupting ARF1-IQGAP1 interaction and ERK signaling

Both HCT116 and RKO cells were exposed to elevating concentrations of LY2839219 (0–3 μM) for transwell assay, showing that LY2839219 decreased the invasion of both CRC cells in a dose dependent manner (Fig. 5A), but not influenced the cell viability (Figure S6A). Notably, the cell invasion of HCT116 and RKO with IQGAP1 knockout was significantly decreased, but refractory to the treatment of LY2839219 (Fig. 5B). Consistently, unlike the control cells, treatment with increasing concentrations of LY2835219 could not decrease p-ERK expression in IQGAP1-knockout HCT116 and RKO cells (Fig. S6B), suggesting that interaction between ARF1 and IQGAP1 is essential for the anticancer bioactivity of LY2839219 in CRC cells. In addition, we observed that LY2839219 treatment abrogated the CRC invasion promoted by ARF1 (Fig. 5C). Even in the RKO-VR cells, the same concentration of LY2839219 (2–3 μM) exhibited comparable inhibitory effect on cell invasion (Fig. 5D). We also employed *in vivo* experimental metastatic model to assess the therapeutic potential of LY2839219. HCT116-Luc cells were intravenously injected into the tail vein of NCG mice and the signal of cell metastasis was observed by bioluminescence imaging. Our result showed that LY2839219 significantly inhibited the lung metastasis of cancer cells (Fig. 5E), which was confirmed by H&E staining (Fig. 5F).

ALT and AST are key serological indicators for assessing liver functions, their upregulation indicates the injury of hepatocyte. In this experiment, no obvious change was found in serum levels of ALT and AST in mice, suggesting that LY2839219 does not cause toxicity (Figure S7). To determine the LY2839219 sensitivity in multiple CRC cells with different levels of ARF1-IQGAP1 interaction, we found that DLD1 exhibited stronger ARF1-IQGAP1 interaction than HCT116 and RKO cells (Figure S6C), and achieved higher the suppressive effect on cell invasion after LY2839219 treatment (Figure S6D). Since LY2839219 is a CDK4/6 inhibitor, we next examined whether other CDK4/6 inhibitor, such as rafoxanide, exerted similar effect on disrupting ARF1-IQGAP1 interaction. As shown in Figure S6E, rafoxanide treatment did not inhibit the interaction of ARF1-IQGAP1, and that knockdown of CDK4 or CDK6 could not eliminate the suppressive effect of LY2839219 on ARF1-IQGAP1 interaction and decrease p-ERK expression (Figure S6F), indicating that the suppressive effect of LY2839219 on ARF1-IQGAP1 interaction dose not rely on CDK4/6. Collectively, interruption of ARF1-IQGAP1 interaction by LY2839219 markedly inhibits CRC metastasis *in vitro* and *in vivo* with no observed side effects.

LY2839219 synergistically improves the anti-metastasis effect of vemurafenib on CRC with high ARF1 expression

Regarding the above findings, we asked whether LY2839219 improves the anticancer effect of vemurafenib in CRC with ARF1 aberrant expression. Our invasion assay demonstrated that combined treatment of LY2839219 and vemurafenib had a synergistical effect on the inhibition of cancer invasion (Fig. 6A), proliferation (Figure S8A), p-ERK (Figure S8B) expression and induction of cell apoptosis (Figure S8C) in HCT116 and RKO cells overexpressing ARF1. To confirm this effect *in vivo*, NCG mice intravenously injected with HCT116-Luc-ARF1 cancer cells were intragastrically administrated with LY2839219, vemurafenib or the combination of LY2839219 and vemurafenib, respectively. Consistent with *in vitro* data, combined treatment of LY2839219 and vemurafenib exerted more suppressive effects on lung metastasis, as compared with control and single treatment groups (Fig. 6B). The metastatic nodes of the lung and kidney in each group were confirmed by H&E staining (Fig. 6C). No noticeable difference in AST and ALT of NCG mice sera was found between the treatment groups and control group (Fig. 6D), suggesting that combined treatment with LY2839219 and vemurafenib is safe to mice. Collectively, our results demonstrate treatment efficacy and safety of LY2839219 as a vemurafenib sensitizer in colorectal cancer.

Fig. 1. ARF1-mediated ERK signaling activation links to vemurafenib resistance and cancer metastasis. (A) Experimental scheme showing the establishment of vemurafenib resistant CRC cell line (RKO-VR) and their invasive ability was compared. The number of invaded cells is shown in the bar chart (B). Scale bar, 100 μm. (C) Transwell invasion assay comparing the invasive ability of RKO and RKO-VR cells with or without vemurafenib treatment (10 μM). Scale bar, 100 μm. (D) Diagram depicting the screening of highly invasive cell lines (RKO-I8 and HCT116-I8). Transwell invasion assay comparing the invasive ability of I8 cells with their corresponding parental cells (E). Scale bar, 100 μm. (F, G) GSEA analysis showing the MAPK signaling pathway was enriched in the DEPs/DEGs of VR and I8 cells. (H) Venn diagram illustrating the overlap of upregulated DEPs/DEGs of RKO-VR and RKO-I8, identifying ARF1 regulating both vemurafenib resistance and cancer invasion. (I) The mRNA level of ARF1 in RKO-VR cells, I8 cells and their corresponding parental cells were analyzed by qRT-PCR. (J, K) Western blotting of the ARF1 and p-ERK levels in HCT116-I8, RKO-I8 and RKO-VR cells compared with their corresponding parental cells. The expression of ARF1 in triplicates was quantified and normalized to corresponding Actin. Bars, SD; **, $P < 0.01$; ***, $P < 0.001$; ns, no significant difference.

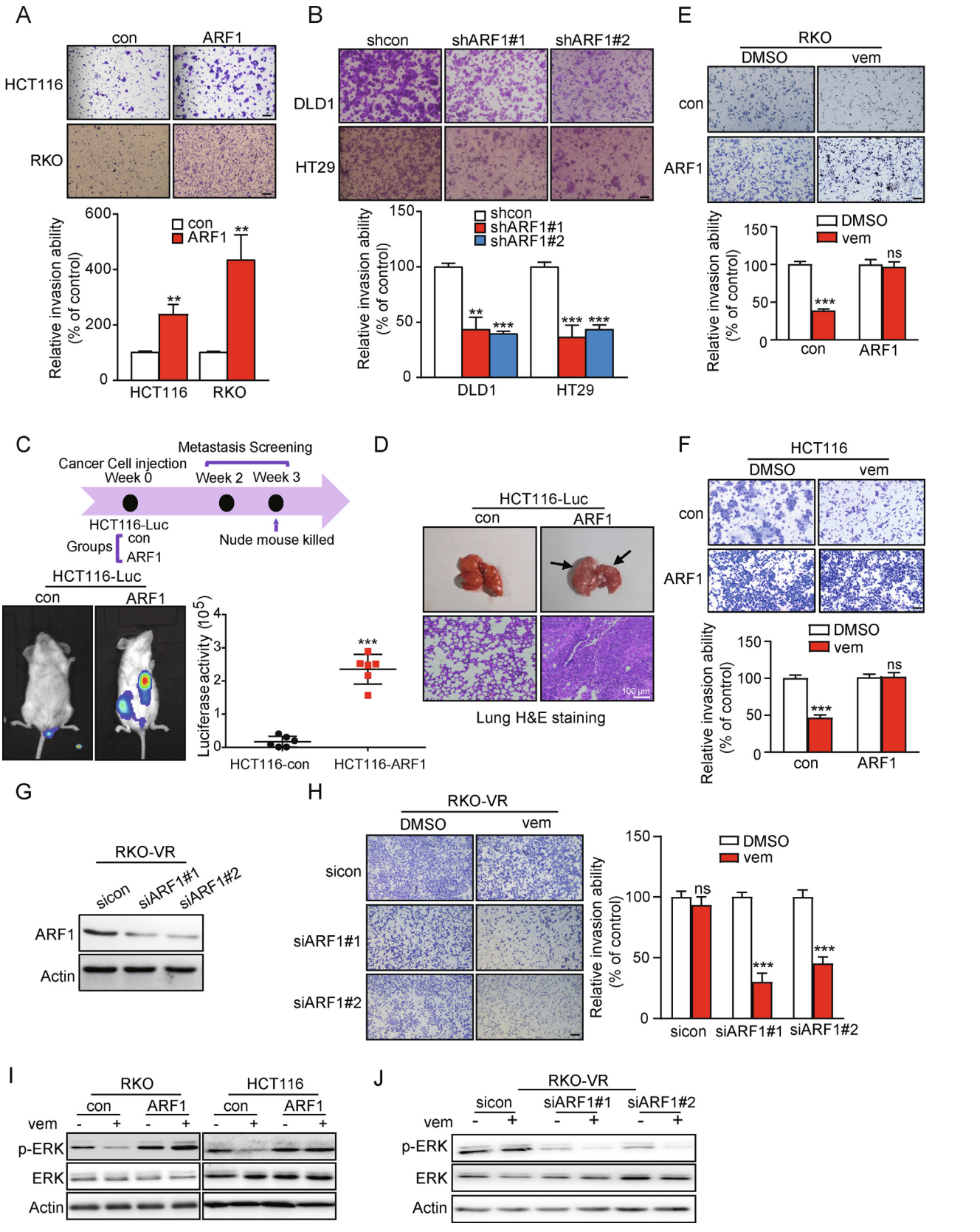
A
con
ARF1
HCT116
RKO
Relative invasion ability (% of control)
600
400
200
0
con
ARF1
**
**
HCT116
RKO
B
shcon
shARF1#1
shARF1#2
DLD1
HT29
Relative invasion ability (% of control)
150
100
50
0
shcon
shARF1#1
shARF1#2
**
***
***
***
DLD1
HT29
E
RKO
DMSO
vem
con
ARF1
Relative invasion ability (% of control)
150
100
50
0
DMSO
vem
***
ns
con
ARF1
C
Metastasis Screening
Cancer Cell injection
Week 0
Week 2
Week 3
HCT116-Luc
Groups
con
ARF1
Nude mouse killed
HCT116-Luc
con
ARF1
Luciferase activity (10^5)
4
3
2
1
0
***
HCT116-con
HCT116-ARF1
D
HCT116-Luc
con
ARF1
100 μm
Lung H&E staining
F
HCT116
DMSO
vem
con
ARF1
Relative invasion ability (% of control)
150
100
50
0
DMSO
vem
***
ns
con
ARF1
G
RKO-VR
sicon
siARF1#1
siARF1#2
ARF1
Actin
H
RKO-VR
DMSO
vem
sicon
siARF1#1
siARF1#2
Relative invasion ability (% of control)
150
100
50
0
DMSO
vem
ns
***
***
sicon
siARF1#1
siARF1#2
I
RKO
HCT116
con
ARF1
con
ARF1
vem
- + - + - + - +
p-ERK
ERK
Actin
J
RKO-VR
sicon
siARF1#1
siARF1#2
vem
- + - + - +
p-ERK
ERK
Actin

Discussion

Drug resistance and tumor metastasis are comment phenomena in late stage of cancer development, which lead to therapy failure and poor clinical outcome of CRC patients. CRC cells with vemurafenib resistance exhibited reactivation of ERK signaling and high invasive capacity. This study discovered that ARF1 has significant expressions to activate MAPK/ERK pathway by interacting with IQGAP1 in vemurafenib-resistant and metastatic CRC and validated that ARF1-IQGAP1 interaction-mediated ERK signaling activation plays a key role in both vemurafenib resistance and metastasis of CRC. In order to target this ARF1-IQGAP1 interaction, we screened out CDK inhibitor LY2839219, an FDA-approved drug, to disrupt the ARF1-IQGAP1 interaction and ERK signaling activation. We further provided *in vitro* and *in vivo* evidences to demonstrate that LY2839219 exerts synergistical anti-metastatic effects on CRC by combination treatment with vemurafenib.

Vemurafenib is a kinase inhibitor of BRAF that achieves satisfactory efficacy in the treatment of metastatic melanoma bearing BRAF-V600E [27]. However, CRC cells continuously exposed to vemurafenib rapidly develop adaptive unresponsiveness [28 9]. Interestingly, we found that our established RKO-VR cell exhibited highly invasive capacity, suggesting that the metastatic ability of CRC cell is acquired and elevated along with the emergence of vemurafenib resistance. Our cell model provides the proof of concept for clinical observation that drug resistance and tumor metastasis are co-occurrent in aggressive CRC. By systematic analyses using proteomics and RNA sequencing, MAPK/ERK signaling was involved in both the vemurafenib resistance and high invasion of CRC. We then validated that phosphorylation of ERK was increased in RKO-VR, RKO-I8 and HCT116-I8 cells, suggesting that VR-mediated ERK reactivation is functioning in CRC metastasis.

ERK signaling pathway plays a key role in cancer metastasis and drug resistance [29–32]. As its main upstream regulator [33,34], BRAF is frequently mutated in CRC, resulting in persistent activation of MEK/ERK signaling in metastasis [34,35]. Long-term suppression of BRAF leads to the reactivation of MEK/ERK signaling, due to the existence of various upstream regulators, such as EGFR, RAS and CRAF [9]. In this connection, this study identified ARF1 as a key regulator in the VR-mediated ERK reactivation of CRC metastasis. ARF1 is a vesicle trafficking associated GTPase that is highly expressed in multiple cancers [36–38]. We also observed previously that ARF1 expression was upregulated in CRC tissues and linked to poor prognosis of CRC patients [15]. Importantly, we here found that ARF1 regulates VR-related ERK signaling *via* the interaction with IQGAP1 in CRC metastasis, suggesting that targeting ARF1-IQGAP1 interaction is an effective strategy for anti-metastatic therapeutics.

Protein-protein interaction plays an essential role in cellular signal transduction, which has been considered as effective targets for drug discovery. Regarding the importance of ARF1-IQGAP1 interaction in cancer metastasis and vemurafenib resistance, we employed our ELISA-based drug screen system to identify LY2839219 as an effective blocker against ARF1-IQGAP1 interaction. LY2839219 is a CDK4/6 inhibitor that widely used for first-line therapy of advanced breast cancer [39]. Clinical trial demonstrated that LY2839219 in combination with fulvestrant remarkably improved median overall survival of breast cancer patients with hormone receptor-positive and ERBB2-negative [40]. Here, we identified a new function of LY2839219 in disrupting ARF1-IQGAP1 interaction independently of CDK4/6 inhibition. LY2839219 overcame the VR-mediated ERK reactivation and cell invasion, and that combination treatment of LY2839219 and vemurafenib exhibited synergistical anti-metastasis effect on CRC, implicating a promising therapeutic strategy for CRC with vemurafenib resistance and metastasis.

Conclusions

Overall, this study uncovers that ARF1-IQGAP1 interaction is involved in vemurafenib resistance mediated ERK signaling reactivation and cancer metastasis, and that LY2835219 is a promising therapeutic agent for aggressive CRC in combination with vemurafenib.

Compliance with Ethics Requirements

The study is approved by the Ethical Review Board of Jinan University. All participants provided written informed consent. All of the animal researches were conducted complying with Guidance for the Care and Use of Laboratory Animals of Jinan University. The study protocol conforms to the ethical guidelines of the 1975 Declaration of Helsinki.

Declaration of Competing Interest

The authors declare that they have no known competing financial interests or personal relationships that could have appeared to influence the work reported in this paper.

Acknowledgments

This work was supported by the National Key Research and Development Program of China (2017YFA0505100, 2020YFE0202200), the National Natural Science Foundation of China (82202842), China Postdoctoral Science Foundation (2021M701418), Guangdong Basic and Applied Basic Research Fund Regional Joint Fund (2021A1515111126).

Fig. 2. ARF1 promotes the vemurafenib resistance and metastasis of CRC. HCT116-con/ARF1, RKO-con/ARF1 (A) and DLD1-shcon/shARF1, HT29-shcon/shARF1 (B) were determined by transwell matrigel invasion assays. Scale bar, 100 μm. The number of invaded cells is shown in the bar chart. (C) Representative bioluminescent images monitoring the cancer metastasis of NCG mice received intravenous injection of indicated cells (HCT116-luc-con or HCT116-luc-ARF1), and the intensity of bioluminescence was quantified. The lungs were harvested for imaging and H&E staining (D). (E, F) Comparison of the invasive ability of RKO-con/ARF1 and HCT116-con/ARF1 treated with or without vemurafenib (10 μM). Scale bar, 100 μm. (G) Western blotting measurement of the protein level of ARF1 in RKO-VR treated with siRNAs. (H) Transwell matrigel invasion assay determining the inhibitory effect of vemurafenib (10 μM) on invasion ability of RKO-VR cells with or without knockdown of ARF1. (I) Western blotting of the protein level of p-ERK and ERK in ARF1-overexpression CRC cells treated with or without vemurafenib (10 μM). (G) Western blotting of the protein level of p-ERK and ERK in ARF1-kncokdown CRC cells treated with or without vemurafenib (10 μM). Scale bar, 100 μm. Bars, SD; *, $P < 0.05$; **, $P < 0.01$; ***, $P < 0.001$; ns, no significant difference.

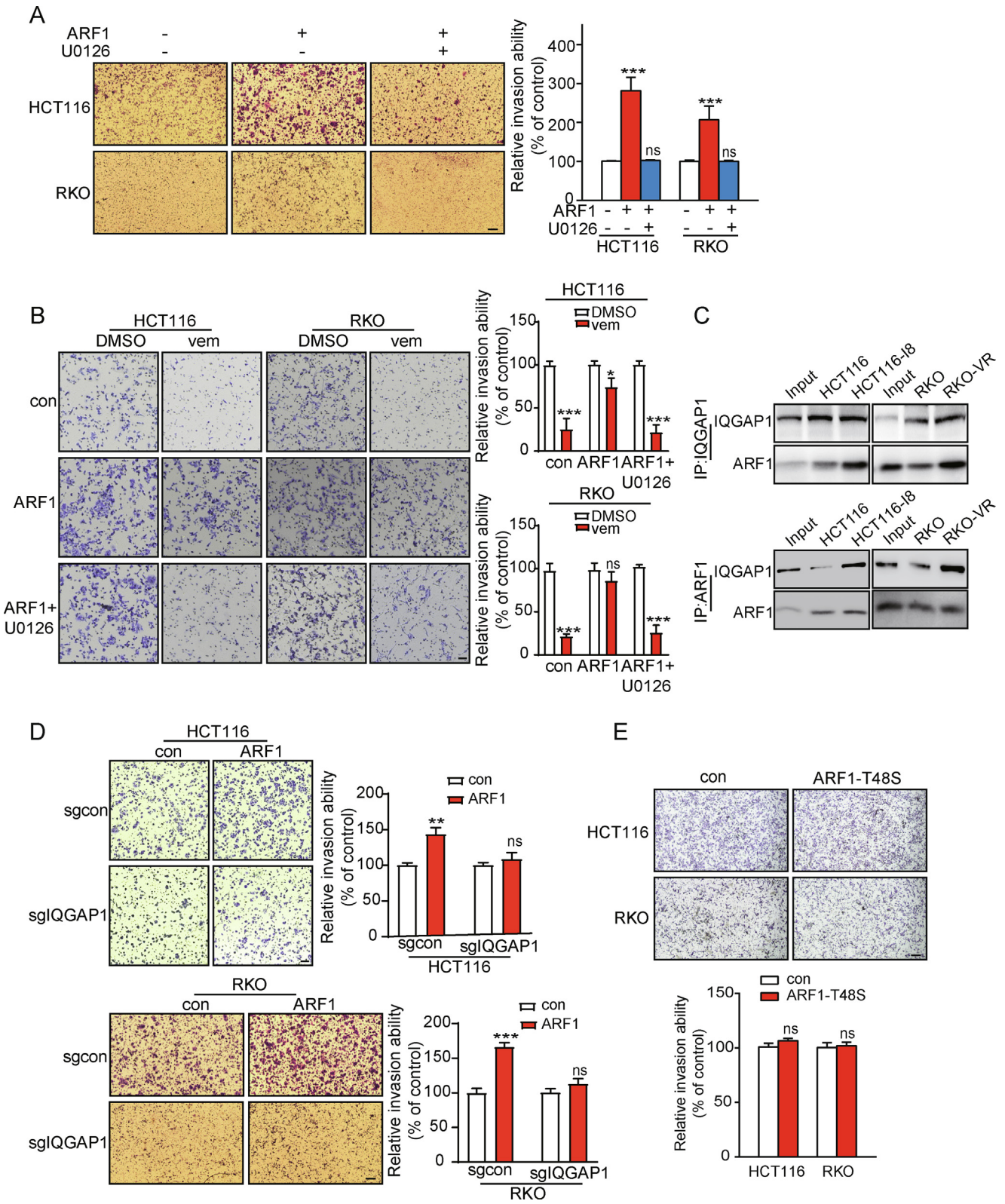

Fig. 3. ARF1 promotes CRC invasion and vemurafenib resistance by activating ERK signaling. (A) Transwell matrigel invasion assay was examined in CRC cells with or without stably expressing ARF1, followed by the treatment of U0126 (10 μM) as indicated. Scale bar, 100 μm. (B) Transwell matrigel invasion assay of CRC cells with indicated treatments. Scale bar, 100 μm. (C) Co-immunoprecipitation assay was performed in HCT116/HCT116-I8 and RKO/RKO-VR cells for analyzing the interaction of ARF1-IQGAP1 by immunoprecipitated IQGAP1. (D) Transwell matrigel invasion assay was performed in HCT116-sgcon/sgIQGAP1 and RKO-sgcon/sgIQGAP1 with or without overexpressing ARF1. Scale bar, 100 μm. (E) Transwell assays were performed to determine invasion of CRC cells with or without overexpressing ARF1-T48S mutant. Scale bar, 100 μm. Bars, SD; *, $P < 0.05$; **, $P < 0.01$; ***, $P < 0.001$; ns, no significant difference.

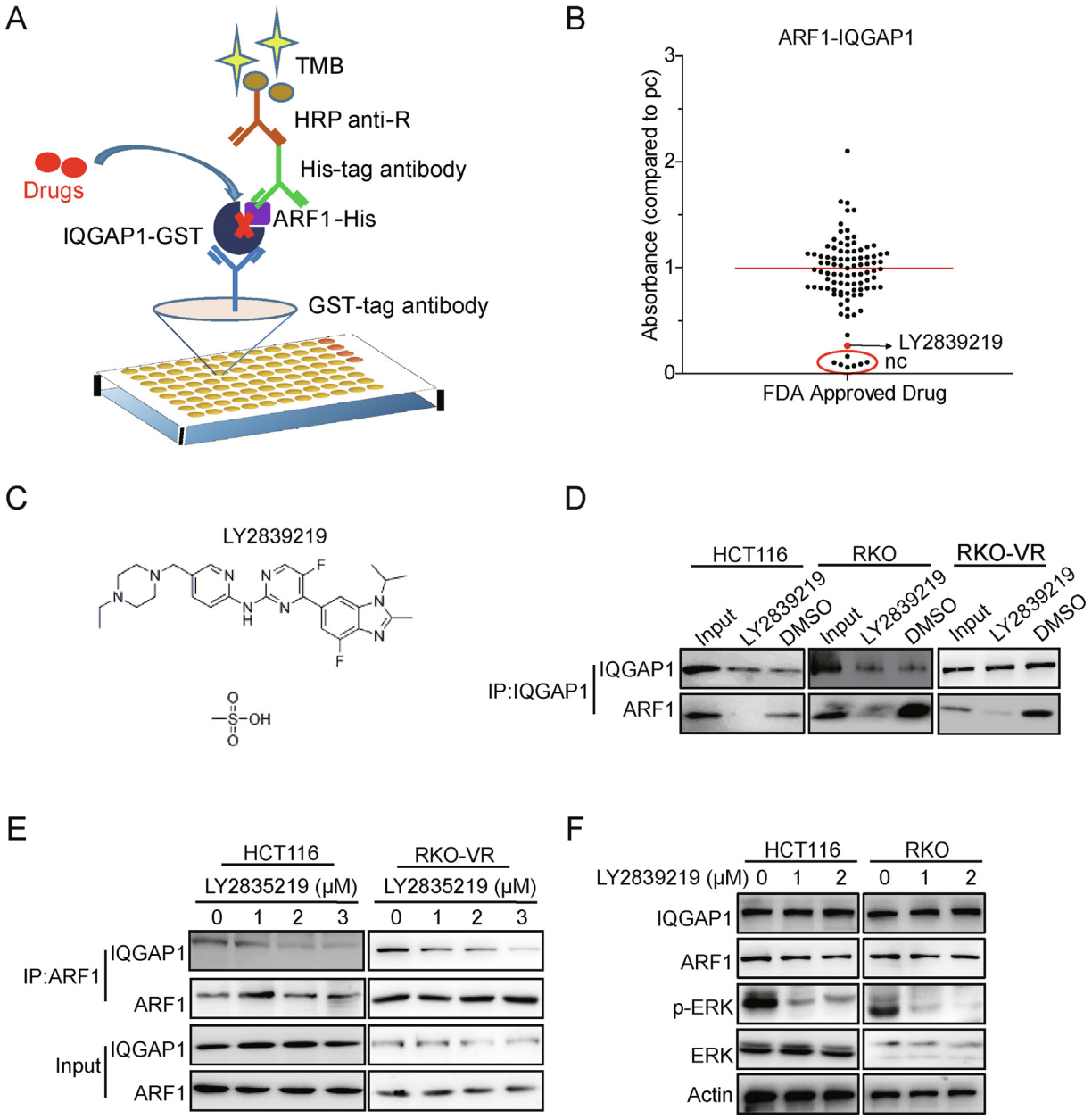

Fig. 4. LY2839219 disrupts the interaction of ARF1-IQGAP1. (A) Experimental scheme of ELISA-based drug screen system using FDA-approved drug library. (B) The absorbance in wells with different drugs treatment. nc, negative control. (C) The structure of LY2839219. (D) Co-immunoprecipitation assay was examined in CRC cells treated with LY2839219 or DMSO for detecting the interaction of ARF1-IQGAP1. (E) Co-precipitation of endogenous ARF1 with IQGAP1 from HCT116 and RKO-VR cells treated with increasing concentrations of LY2839219 (0–3 μM). (F) Western blotting measurement of the protein level of IQGAP1, ARF1, p-ERK and ERK expression in HCT116 and RKO treated with elevating concentration of LY2839219.

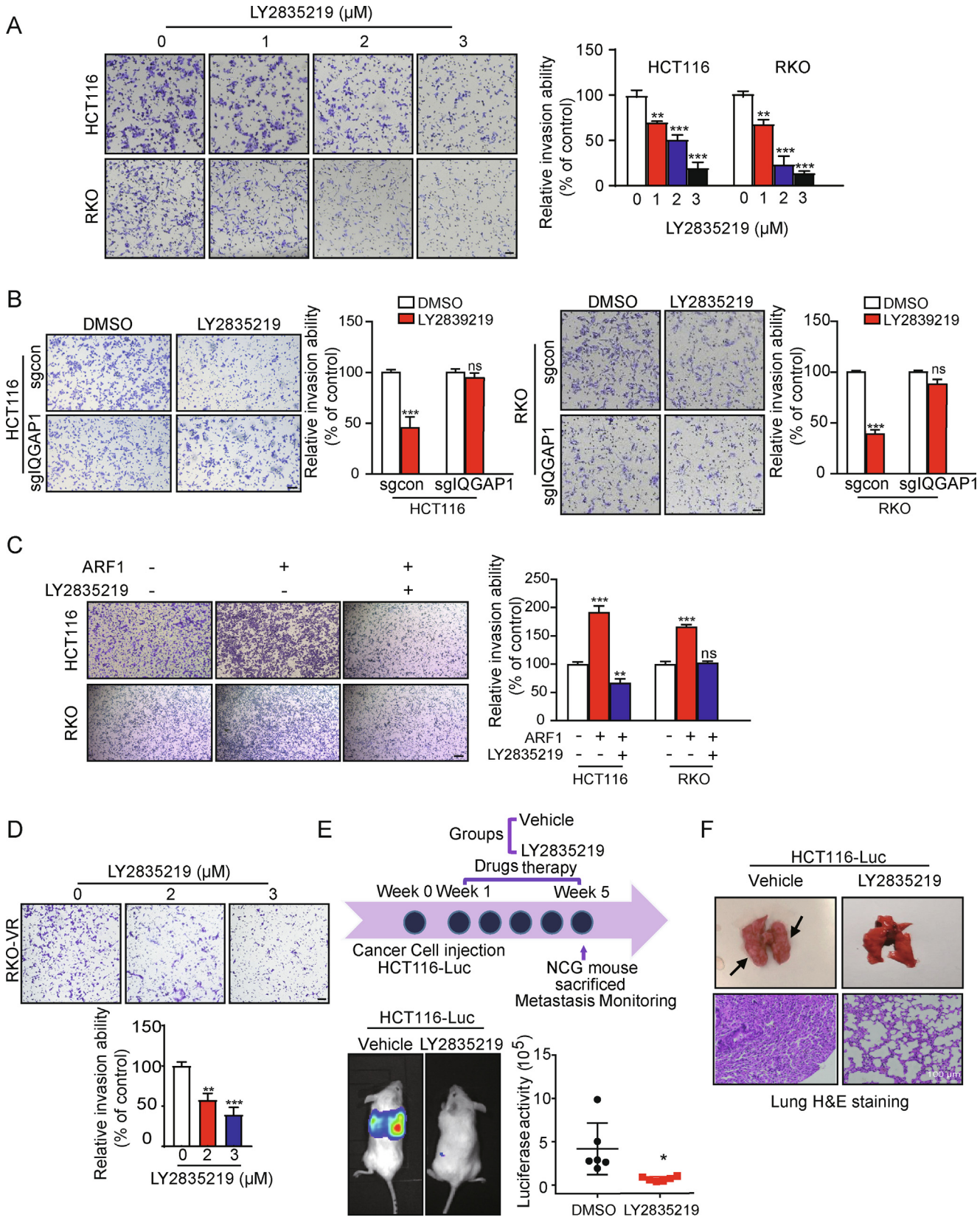

Fig. 5. LY2839219 suppresses CRC metastasis *in vivo* and *in vitro*. (A) Transwell matrigel invasion assay of HCT116 and RKO cells treated with elevating concentration of LY2839219. Scale bar, 100 μm. (B) The invasive ability of HCT116-sgcon/HCT116-sgIQGAP1 and RKO-sgcon/RKO-sgIQGAP1 treated with or without LY2839219 (2 μM). Scale bar, 100 μm. (C) Invasive ability of ARF1-overexpressing CRC cells treated with or without LY2839219 (2 μM) were compared with control cells. Scale bar, 100 μm. (D) Transwell assay comparing the invasion of RKO-VR cells treated with LY2839219 (2–3 μM) and DMSO. Scale bar, 100 μm. (E) Representative bioluminescent images monitoring the cancer metastasis in NCG mice received intravenous injection of HCT116-Luc-ARF1 cells treated with or without LY2839219 (5 mg/kg), and the intensity of bioluminescence was quantified. (F) The lungs were harvested for imaging and H&E staining. Scale bar, 100 μm. Bars, SD; *, $P < 0.05$; **, $P < 0.01$; ***, $P < 0.001$; ns, no significant difference.

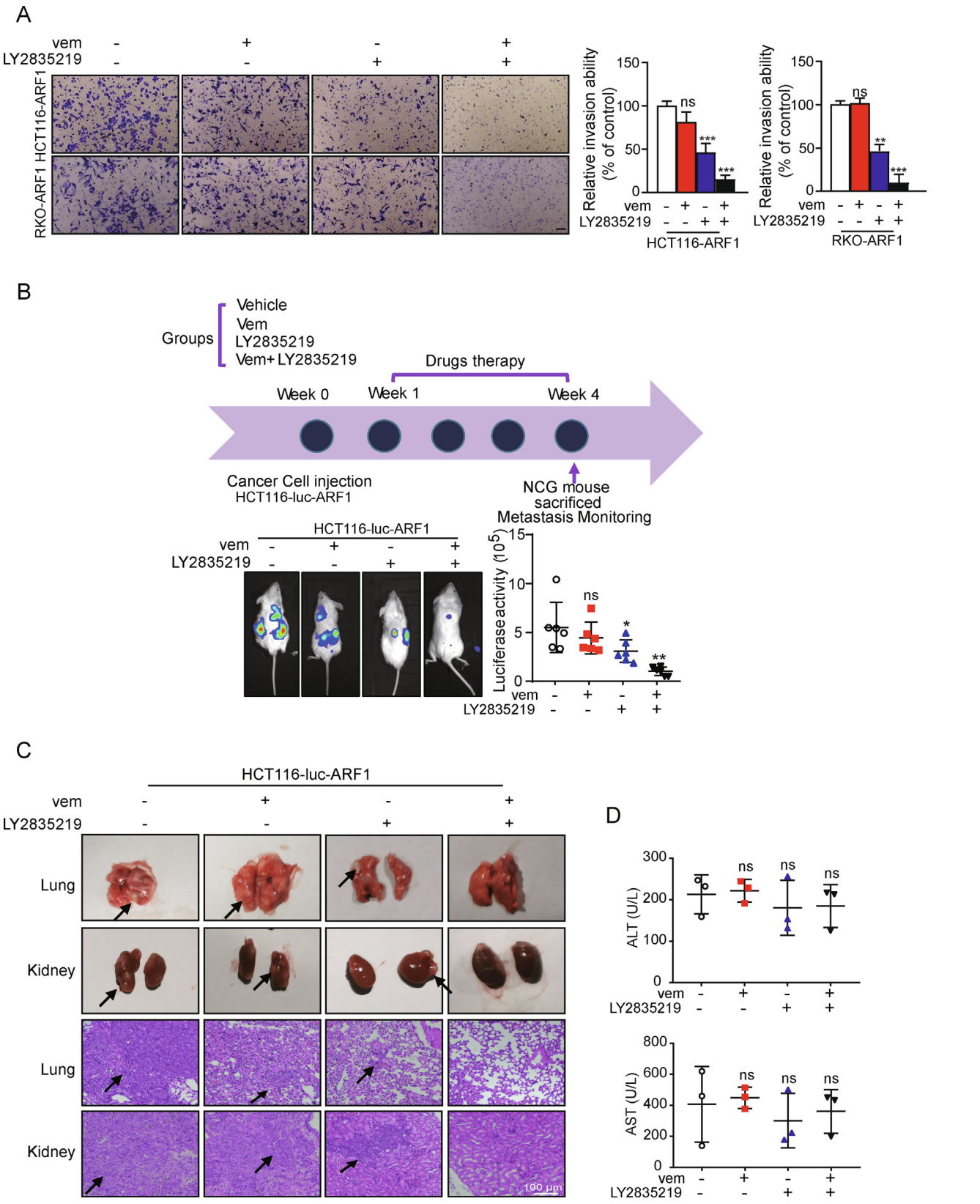

Fig. 6. Combination of LY2839219 and vemurafenib significantly inhibits ARF1-mediated cancer metastasis. (A) Transwell matrigel invasion assay was used in HCT116-ARF1 and RKO-ARF1 cells treated with or without the combined use of LY2839219 and vemurafenib. Scale bar, 100 μm. (B) Combined treatment of LY2839219 with vemurafenib suppressed CRC metastasis *in vivo*. Upper panel, diagram depicting the drugs treatment. Down panel, cancer metastasis in NCG mice was detected by bioluminescent images and quantified. The lung and kidney were harvested for imaging and H&E staining of the metastatic nodes (C). (D) ALT and AST were analyzed in mice serum. Bars, SD; *, $P < 0.05$; **, $P < 0.01$; ***, $P < 0.001$.

Appendix A. Supplementary material

Supplementary data to this article can be found online at https://doi.org/10.1016/j.jare.2022.11.006.

References

[1] Sung H, Ferlay J, Siegel RL, Laversanne M, Soerjomataram I, Jemal A, *et al.* **Global Cancer Statistics 2020: GLOBOCAN Estimates of Incidence and Mortality Worldwide for 36 Cancers in 185 Countries**. CA: a cancer journal for clinicians, **71**(3)(2021), pp.209-249.

[2] Weinberg BA, Marshall JL, Salem ME. The growing challenge of young adults with colorectal cancer. Oncol (Williston Park, NY) 2017;31(5):381–9.

[3] Chen W, Zheng R, Baade PD, Zhang S, Zeng H, Bray F, *et al.* **Cancer statistics in China, 2015**. CA: a cancer journal for clinicians, **66**(2)(2016), pp.115-132.

[4] Biller LH, Schrag D. Diagnosis and Treatment of Metastatic Colorectal Cancer: A Review. JAMA 2021;325(7):669–85.

[5] Acharyya S, Oskarsson T, Vanharanta S, Malladi S, Kim J, Morris PG, et al. A CXCL1 paracrine network links cancer chemoresistance and metastasis. Cell 2012;150(1):165–78.

[6] Yao Z, Torres NM, Tao A, Gao Y, Luo L, Li Q, et al. BRAF Mutants Evade ERK-dependent feedback by different mechanisms that determine their sensitivity to pharmacologic inhibition. Cancer Cell 2015;28(3):370–83.

[7] Tiacci E, De Carolis L, Simonetti E, Capponi M, Ambrosetti A, Lucia E, et al. Vemurafenib plus Rituximab in Refractory or Relapsed Hairy-Cell Leukemia. The New England j med 2021;384(19):1810–23.

[8] Yukimoto R, Nishida N, Hata T, Fujino S, Ogino T, Miyoshi N. Specific activation of glycolytic enzyme enolase 2 (ENO2) in BRAF V600E-mutated colorectal cancer. Cancer Sci 2021.

[9] Prahallad A, Sun C, Huang S, Di Nicolantonio F, Salazar R, Zecchin D, et al. Unresponsiveness of colon cancer to BRAF(V600E) inhibition through feedback activation of EGFR. Nature 2012;483(7387):100–3.

[10] Corcoran RB, Ebi H, Turke AB, Coffee EM, Nishino M, Cogdill AP, et al. EGFR-mediated re-activation of MAPK signaling contributes to insensitivity of BRAF mutant colorectal cancers to RAF inhibition with vemurafenib. Cancer discovery 2012;2(3):227–35.

[11] Lang L, Shay C, Zhao X, Teng Y. Combined targeting of Arf1 and Ras potentiates anticancer activity for prostate cancer therapeutics. Journal of experimental & clinical cancer research : CR, **36**(1)(2017), pp.112.

[12] Schlienger S, Campbell S, Claing A. ARF1 regulates the Rho/MLC pathway to control EGF-dependent breast cancer cell invasion. Mol Biol Cell 2014;25(1):17–29.

[13] Lewis-Saravalli S, Campbell S, Claing A. ARF1 controls Rac1 signaling to regulate migration of MDA-MB-231 invasive breast cancer cells. Cell Signal 2013;25(9):1813–9.

[14] Luchsinger C, Aguilar M, Burgos PV, Ehrenfeld P, Mardones GA. **Functional disruption of the Golgi apparatus protein ARF1 sensitizes MDA-MB-231 breast cancer cells to the antitumor drugs Actinomycin D and Vinblastine through ERK and AKT signaling**. PloS one, **13**(4)(2018), pp.e0195401.

[15] Hu HF, Xu WW, Li YJ, He Y, Zhang WX, Liao L, et al. Anti-allergic drug azelastine suppresses colon tumorigenesis by directly targeting ARF1 to inhibit IQGAP1-ERK-Drp1-mediated mitochondrial fission. Theranostics 2021;11(4):1828–44.

[16] Yang J, Xu WW, Hong P, Ye F, Huang XH, Hu HF, et al. Adefovir dipivoxil sensitizes colon cancer cells to vemurafenib by disrupting the KCTD12-CDK1 interaction. Cancer Lett 2019;451:79–91.

[17] Rugo HS, O'Shaughnessy J, Boyle F, Toi M, Broom R, Blancas I, et al. Adjuvant Abemaciclib Combined with Endocrine Therapy for High Risk Early Breast Cancer: Safety and Patient-Reported Outcomes From the monarchE Study. Annals of oncology : official journal of. the European Society for Medical Oncology; 2022.

[18] Corona SP, Generali D. Abemaciclib: a CDK4/6 inhibitor for the treatment of HR+/HER2- advanced breast cancer. Drug design, development and therapy 2018;12:321–30.

[19] Hu HF, Xu WW, Wang Y, Zheng CC, Zhang WX, Li B. Comparative Proteomics Analysis Identifies Cdc42-Cdc42BPA signaling as prognostic biomarker and therapeutic target for colon cancer invasion. J Proteome Res 2018;17(1):265–75.

[20] Hu HF, Xu WW, Zhang WX, Yan X, Li YJ, Li B, *et al.* **Identification of miR-515-3p and its targets, vimentin and MMP3, as a key regulatory mechanism in esophageal cancer metastasis: functional and clinical significance**. Signal transduction and targeted therapy, **5**(1)(2020), pp.271.

[21] Sun Y, Yang YM, Hu YY, Ouyang L, Sun ZH, Yin XF, et al. Inhibition of nuclear deacetylase Sirtuin-1 induces mitochondrial acetylation and calcium overload leading to cell death. Redox Biol 2022;53:102334.

[22] Wang Y, Zhang J, Li YJ, Yu NN, Liu WT, Liang JZ, *et al.* **MEST promotes lung cancer invasion and metastasis by interacting with VCP to activate NF-κB signaling**. Journal of experimental & clinical cancer research : CR, **40**(1)(2021), pp.301.

[23] Wang Y, Zhang J, Zhong LY, Huang SJ, Yu NN, Ouyang L, et al. Hsa-miR-335 enhances cell migration and invasion in lung adenocarcinoma through targeting Copine-1. MedComm 2021;2(4):810–20.

[24] Hu HF, Xu WW, Wang Y, Zheng CC, Zhang WX, Li B. Comparative Proteomics Analysis Identifies Cdc42-Cdc42BPA signaling as prognostic biomarker and. Therapeutic Target for Colon Cancer Invasion 2018;17(1):265–75.

[25] Zhou F, Dong C, Davis JE, Wu WH, Surrao K, Wu G. The mechanism and function of mitogen-activated protein kinase activation by ARF1. Cell Signal 2015;27(10):2035–44.

[26] Meierhofer T, Eberhardt M, Spoerner M. Conformational states of ADP ribosylation factor 1 complexed with different guanosine triphosphates as studied by 31P NMR spectroscopy. Biochemistry 2011;50(29):6316–27.

[27] Bollag G, Hirth P, Tsai J, Zhang J, Ibrahim PN, Cho H, et al. Clinical efficacy of a RAF inhibitor needs broad target blockade in BRAF-mutant melanoma. Nature 2010;467(7315):596–9.

[28] Wang Z, Ye CY. The Role of Dynamic ctDNA monitoring during combination therapies of BRAF V600E-mutated metastatic colorectal cancer: a case report. OncoTargets and therapy 2020;13:11849–53.

[29] Zhang F, Zhu X, Wang P, He Q, Huang H, Zheng T, *et al.* **The cytokine FAM3B/PANDER is an FGFR ligand that promotes posterior development in Xenopus**. Proceedings of the National Academy of Sciences of the United States of America, **118**(20)(2021).

[30] Cronin R, Brooke GN. The role of the p90 ribosomal S6 kinase family in prostate cancer progression and therapy resistance. Oncogene 2021.

[31] Ni QF, Yu JW, Qian F, Sun NZ, Xiao JJ, Zhu JW. Cortactin promotes colon cancer progression by regulating ERK pathway. Int J Oncol 2015;47(3):1034–42.

[32] Wang Y, Zhang J, Zheng CC, Huang ZJ, Zhang WX, Long YL, *et al.* **C20orf24 promotes colorectal cancer progression by recruiting Rin1 to activate Rab5-mediated mitogen-activated protein kinase/extracellular signal-regulated kinase signalling**. Clinical and translational medicine, **12**(4)(2022), pp.e796.

[33] Zhou Y, Li Z, Wu X, Tou L, Zheng J, Zhou D. MAGOH/MAGOHB Inhibits the Tumorigenesis of Gastric Cancer via Inactivation of b-RAF/MEK/ERK Signaling. OncoTargets and therapy 2020;13:12723–35.

[34] Chiu CF, Ho MY, Peng JM, Hung SW, Lee WH, Liang CM, et al. Raf activation by Ras and promotion of cellular metastasis require phosphorylation of prohibitin in the raft domain of the plasma membrane. Oncogene 2013;32(6):777–87.

[35] Kim N, Shin I. **Novel and Potent Small Molecules against Melanoma Harboring BRAF Class I/II/III Mutants for Overcoming Drug Resistance**. International journal of molecular sciences, **22**(7)(2021).

[36] Xu X, Wang Q, He Y, Ding L, Zhong F, Ou Y, et al. ADP-ribosylation factor 1 (ARF1) takes part in cell proliferation and cell adhesion-mediated drug resistance (CAM-DR). Ann Hematol 2017;96(5):847–58.

[37] Luchsinger C, Aguilar M, Burgos PV, Ehrenfeld P, Mardones GA. **Functional disruption of the Golgi apparatus protein ARF1 sensitizes MDA-MB-231 breast cancer cells to the antitumor drugs Actinomycin D and Vinblastine through ERK and AKT signaling**. **13**(4)(2018), pp.e0195401.

[38] Schlienger S, Ramirez RA, Claing A. ARF1 regulates adhesion of MDA-MB-231 invasive breast cancer cells through formation of focal adhesions. Cell Signal 2015;27(3):403–15.

[39] Braal CL, Jongbloed EM, Wilting SM, Mathijssen RHJ, Koolen SLW, Jager A. Inhibiting CDK4/6 in Breast Cancer with Palbociclib, Ribociclib, and Abemaciclib: Similarities and Differences. Drugs 2021;81(3):317–31.

[40] Sledge Jr GW, Toi M, Neven P, Sohn J, Inoue K, Pivot X, et al. The Effect of Abemaciclib Plus Fulvestrant on Overall Survival in Hormone Receptor-Positive, ERBB2-Negative Breast Cancer That Progressed on Endocrine Therapy-MONARCH 2: a Randomized Clinical Trial. JAMA oncology 2020;6(1):116–24.